THIELE CENTRE
FOR APPLIED MATHEMATICS IN NATURAL SCIENCE

Estimating the Euler Characteristic of a planar set from a digital image

Markus Kiderlen

06

Research Report

No. 03 | January 2006

Estimating the Euler Characteristic of a planar set from a digital image

This Thiele Research Report is also Research Report number 471 in the Stochastics Series at Department of Mathematical Sciences, University of Aarhus, Denmark.

Estimating the Euler Characteristic of a planar set from a digital image

Markus Kiderlen

Department of Mathematical Sciences, University of Aarhus, Denmark

Abstract

A new estimator (approximation) for the Euler-Poincaré characteristic of a planar set K in the extended convex ring is suggested. As input, it uses only the digital image of K, which is modeled as the set of all points of a regular lattice falling in K. The key idea is to estimate the two planar Betti numbers of K (number of connected components and number of holes) by approximating K and its complement by polygonal sets derived from the digitization. In contrast to earlier methods, only certain connected components of these approximations are counted. The estimator of the Euler characteristic is then defined as the difference of the estimators for the two Betti numbers. Under rather weak regularity assumptions on K, it is shown that all three estimators yield the correct result, whenever the resolution of the image is sufficiently high.

Key words: Euler Characteristic, digital morphology, convex ring, digitized image, multigrid convergence, Betti number
1991 MSC: 68U10, 52C05

1 Introduction and main result

The Euler-Poincaré characteristic (Euler characteristic for short) describes the connectivity properties of the components of a composite material. It is used in such disparate applied areas as medicine to characterize cancellous bone (Boyce *et al.* [1]), in statistical physics to describe morphological properties of fluids (Mecke [2]), and in material sciences to analyze foams and other porous media (Levitz [3]). By means of the Crofton formula, the estimation of the Euler characteristic, applied to sections of the structure, can be used to estimate the other intrinsic volumes, like surface area, volume or curvature integrals; see e.g. Schneider & Weil [4]. It is, however, nontrivial to estimate the Euler characteristic $\chi(K)$ of a structure K

Email address: kiderlen@imf.au.dk (Markus Kiderlen).
[1] Supported by the Carlsberg Foundation.

from digital images, even if the structure is planar. The purpose of this paper is to present a new estimator of $\chi(K)$ and to show that this estimator yields the correct result, whenever the resolution of the digital image is high enough. The required regularity assumptions on K are hereby relatively weak. We emphasize in this work, in contrast to many of the earlier contributions, the interplay between "continuous" and "digitized" world.

We think of K as being a subset of two-dimensional space $\mathbb{R}^2$ and make the usual assumption that $K \in \mathcal{R}$, where the *convex ring* $\mathcal{R}$ consists of all finite unions of *convex bodies* (compact convex sets) in $\mathbb{R}^2$. In general dimensions, the *Euler characteristic* can be written as alternating sum of Betti numbers. In the plane, we have

$$\chi(K) = N_c(K) - N_h(K), \qquad K \in \mathcal{R}, \tag{1}$$

where $N_c(K)$ is the *number of connected components of* K and $N_h(K)$ is the *number of its holes* (bounded connected components of the complement of K). The information on K available for the estimation of $\chi(K)$ is very weak here. It only consists of a *digital 0-1-image* (or *digitization*), which is modeled as the intersection of K with a *regular lattice*

$$\mathbb{L} = \{n_1x_1 + n_2x_2 \mid n_1, n_2 \in \mathbb{Z}\}, \tag{2}$$

generated by a basis x_1, x_2 of $\mathbb{R}^2$. Often the standard lattice $\mathbb{L} = \mathbb{Z}^2$ is chosen. (Klette & Rosenfeld [5] call $K \cap \mathbb{Z}^2$ the *Gauss digitization*, where the lattice points are the centers of the image pixels.) The set

$$\mathsf{C}_0 = \{\alpha_1x_1 + \alpha_2x_2 \mid 0 \leqslant \alpha_1, \alpha_2 \leqslant 1\}$$

is called a *closed unit cell of* $\mathbb{L}$. Known approaches to estimate $\chi(K)$ from a digitization of K can be assorted in three groups, which differ in their theoretical foundation, but turn out to be equivalent in many respects, see Section 2, below.

a) Graph theoretic approach; see e.g. Serra [6] and Rosenfeld & Kak [7, Section 9.1]. A neighbourhood relation on $K \cap \mathbb{L}$ and a neighbourhood graph $\mathcal{G}(K)$ with vertex set $K \cap \mathbb{L}$ and edges connecting all neighbouring vertices are introduced. The Euler characteristic of K is then estimated by the graph theoretic Euler characteristic of $\mathcal{G}(K)$.

   One of the most common neighbourhood relations is the so-called *4-neighbourhood*. Two lattice points $p, q \in \mathbb{L}$ are considered 4-neighbours, if they are "horizontal" or "vertical" neighbours (i.e. $p - q \in \{\pm x_1, \pm x_2\}$). If, in addition, "diagonal" neighbours ($p - q \in \{\pm(x_1 + x_2), \pm(x_1 - x_2)\}$) are admitted, the *8-neighbourhood* with corresponding neighbourhood graph $\mathcal{G}_8(K)$ is obtained. Other neighbourhoods (Serra [6, p. 174], Heijmans [8, p. 327]) are also in use, we only mention the common *6-neighbourhood* (based on a hexagonal-II graph), which differs from the *8-neighbourhood* by omitting two diagonal neighbours aligned with p.

b) Polyhedral approach. A set $\mathcal{P}$ of polygons in C_0 ("basic bricks") with vertices in $\mathbb{L}$ and some additional properties is fixed. A polygonal approximation P of K is obtained as the union of all those translations of sets in $\mathcal{P}$ that have all their vertices in $K \cap \mathbb{L}$. The Euler characteristic $\chi(P)$ of P is then considered as an estimator for $\chi(K)$.

Typical choices for $\mathcal{P}$ are the family $\mathcal{P}_4$ containing all faces of the closed unit cell C_0 (4 vertices, 4 edges and C_0 itself), and the family $\mathcal{P}_8$ of all polygons with vertices in $\{o, x_1, x_2, x_1+x_2\}$. Detailed definitions, including the important notion of *adjacency system*, further examples and properties are discussed by Ohser *et al.* [9], [10]. A variant of this approach is the approximation of K by a set S with smooth boundary and to use $\chi(S)$ as an estimator. This was made precise by Lee *et al.* [11]. Depending on the smoothing procedure, this leads to the same results as polygonal approximation based on $\mathcal{P}_4$ or $\mathcal{P}_8$.

c) Integral geometric approach. This approach, suggested by Ohser & Nagel [12], discretizes the recursive definition of the Euler characteristic given by Hadwiger [13]. It uses the fact that there is a natural estimator for χ of sets in $\mathbb{R}^1$ and derives an estimator for sets in $\mathbb{R}^2$ by comparing pairs of sections of K with parallel lines. These lines are close to one another and lie in lattice directions.

As the only available information on K is the (finite) set $K \cap \mathbb{L}$, it is not amazing that no estimator $\hat{\chi}_{\mathbb{L}}(\cdot)$ can yield the correct Euler characteristic for all sets $K \in \mathcal{R}$. A reasonable requirement is, however, that the estimator converges to $\chi(K)$ if the lattice becomes finer and finer, i.e. if $K \cap t\mathbb{L}$ is observed, where the scaling factor $t > 0$ converges to 0. Let $\mathcal{M} \subset \mathcal{R}$ be some family of planar sets. Let ϕ be some real valued functional on $\mathcal{R}$. Following Klette & Rosenfeld [5, p. 70], we call an estimator $\hat{\phi}_{t\mathbb{L}}$ *multigrid convergent to ϕ for $\mathcal{M}$*, if

$$\lim_{t \to 0_+} \hat{\phi}_{t\mathbb{L}}(K \cap t\mathbb{L}) = \phi(K) \quad \text{for all } K \in \mathcal{M}. \tag{3}$$

Note, however, that the dependence of $\hat{\phi}_{t\mathbb{L}}$ on $t\mathbb{L}$ is not made explicit in [5, p. 70], which is misleading in a general context. Heijmans [8, Definition 8.11] introduces the notion of a discretization of an operator, which is closely related to the above. More precisely, if (3) holds, then $\{\hat{\phi}_{1/n\mathbb{L}}\}_{n \geqslant 1}$ is a *(operator-)discretization of ϕ on $\mathcal{M}$* with respect to the (set-)discretization $\{1/n\mathbb{L}, \sigma_n, \varrho_n\}$. Here $\sigma_n : K \mapsto K \cap 1/n\mathbb{L}$, ϱ_n is the identity on $1/n\mathbb{L}$ and we extended Heijman's definition allowing subclasses $\mathcal{M}$ of the family of *all* planar closed subsets. If $\phi(K)$ is always an integer, like in the case of the Euler characteristic and of the Betti numbers considered before, multigrid convergence can be reformulated as follows. If $\hat{\phi}_{\mathbb{L}}$ satisfies (3) for some set class $\mathcal{M}$ and $x \mapsto [x]$ denotes the nearest integer function (round off), then $\left[\hat{\chi}_{\mathbb{L}}(\cdot)\right]$ is an integer valued multigrid convergent estimator to ϕ for $\mathcal{M}$. Hence there is a constant $t(K) > 0$ depending on K, such that

$$\left[\hat{\phi}_{t\mathbb{L}}(K \cap t\mathbb{L})\right] = \phi(K), \qquad 0 < t \leqslant t(K). \tag{4}$$

Therefore, finding a multigrid convergent estimator of χ, N_c and N_h is equivalent of finding an estimator, which gives the exact value for sufficiently small lattice spacing. All the estimators in the present paper are integer valued.

As lower dimensional parts of a set $K \in \mathcal{R}$ are typically not visible in the digitization, the estimators in a), b) and c) cannot be multigrid convergent for $\mathcal{R}$. But even if we restrict considerations to sets without lower dimensional parts (topological regular sets) multigrid convergence does not hold. This is amazing at first glance, as all the estimators in a), b) and c) are geometrically motivated. Mathematically, however, this is easily explained by the fact that the Euler characteristic is not a continuous functional on $\mathcal{R}$. For instance, even though the polygonal approximation in b) converges to K in the Hausdorff-metric under mild assumptions on K, its Euler characteristic need not converge. Figure 1 shows a simple counterexample, where K is even convex and has interior points, i.e. K is a element of the family $\mathcal{K}_0$ of full-dimensional convex bodies in $\mathbb{R}^2$.

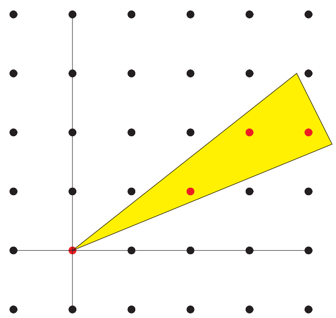

Fig. 1. The digitization of K consists of 4 points. The methods a), b) and c) all treat the origin as an isolated point and yield $\hat{\chi}_{\mathbb{L}}(K \cap \mathbb{L}) \geqslant 2$ as an estimator for $\chi(K) = 1$. The same situation occurs, when $\mathbb{L}$ is replaced by $2^{-k}\mathbb{L}$ with $k = 1, 2, 3, \ldots$, which shows that multigrid convergence does not hold for this triangle.

We will introduce a new estimator for the Euler characteristic being multigrid convergent for $\mathcal{M} = \tilde{\mathcal{R}}$, where the class $\tilde{\mathcal{R}}$ is only slightly smaller than $\mathcal{R}$ and contains in particular $\mathcal{K}_0$.

Definition 1 *Let $\tilde{\mathcal{R}}$ be the family of all nonempty $K \subset \mathbb{R}^2$ with a representation $K = \bigcup_{i=1}^m K_i$ with convex bodies $K_1, \ldots, K_m$ such that*

(i) for all $\emptyset \neq I \subset \{1, \ldots, m\}$ the set $\bigcap_{i \in I} K_i$ is empty or has interior points,
(ii) for all $i \neq j \in \{1, \ldots, m\}$ the intersection $\partial K_i \cap \partial K_j$ of the boundaries of K_i and K_j is finite.

The intersection regularity (i) avoids touching situations of the constituents of K, which are typically misleading in the interpretation of the digitization. The second condition is more technical, but together with (i) it guarantees that any set in $\tilde{\mathcal{R}}$ can locally be written as the union of at most two convex bodies; see Lemma 2 in Section 3, below. This property essentially reduces a multigrid convergence proof for arbitrary $K \in \tilde{\mathcal{R}}$ to one for unions of only *two* convex bodies.

Like in b) we will work with polygonal approximation, but base our estimator of χ on (1). Let $[a, b]$ be the line segment with endpoints $a, b \in \mathbb{R}^2$. Put

$$\mathcal{P}_0 = \{\mathsf{C}_0\} \cup \{[a, b] \mid a \neq b,\ a, b \in \operatorname{vert} \mathsf{C}_0\},$$

where vert P is the set of vertices of a polygon P (and hence vert $\mathsf{C}_0 = \{o, x_1, x_2, x_1 + x_2\}$). The polygonal approximation, based on $\mathcal{P}_0$ and $K \cap t\mathbb{L}$ is defined by

$$\hat{P}_t = \bigcup_{x \in t\mathbb{L}} \bigcup_{\substack{F \in t\mathcal{P}_0 \\ \mathrm{vert}(x+F) \subset K \cap t\mathbb{L}}} (x + F). \tag{5}$$

As polygonal approximation for the complement of K, we use

$$\hat{Q}_t = \bigcup_{x \in t\mathbb{L}} \bigcup_{\substack{F \in t\mathcal{P}_0 \\ \mathrm{vert}(x+F) \subset (K \cap t\mathbb{L})^C}} (x + F). \tag{6}$$

To correct for degenerate cases like in Figure 1, we do not work with the numbers of connected components of $\hat{P}_t$ and $\hat{Q}_t$ directly. Instead, for $P \in \mathcal{R}$ let $\hat{N}_c(P)$ be the number of connected components of P *containing interior points*. In Figure 2 a simple example is given. With these notions at hand, we can state our main result.

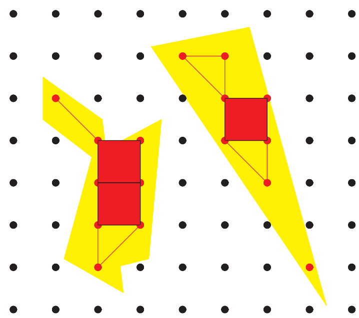

Fig. 2. An example illustrating the definition of $\hat{N}_c(\hat{P}_t)$. The set K is light gray. The number of connected components of its polygonal approximation $\hat{P}_t$ (in dark-gray, including one isolated lattice point in the lower right) is 3, but $\hat{N}_c(\hat{P}_t) = 2$.

Theorem 1 *Let a regular lattice $\mathbb{L}$ and $K \in \tilde{\mathcal{R}}$ be given. If $\hat{P}_t$ and $\hat{Q}_t$ are given by* (5) *and* (6), *respectively, then*

$$\hat{N}_c(\hat{P}_t), \quad \hat{N}_c(\hat{Q}_t) - 1, \quad \text{and} \quad \hat{\chi}_t = \hat{N}_c(\hat{P}_t) - (\hat{N}_c(\hat{Q}_t) - 1)$$

are multigrid convergent estimators for $N_c(K)$, $N_h(K)$ and $\chi(K)$, respectively.

In other words, there is a constant $t_K > 0$ such that for all $0 < t < t_K$ we have

$$\hat{N}_c(\hat{P}_t) = N_c(K), \;\; \hat{N}_c(\hat{Q}_t) - 1 = N_h(K), \;\; \text{and} \; \hat{N}_c(\hat{P}_t) - (\hat{N}_c(\hat{Q}_t) - 1) = \chi(K).$$

Note that $\hat{N}_c(\hat{Q}_t)$ is an estimator of the number of connected components of K^C, so we have to subtract 1 (for the one component that is unbounded) to obtain the number of holes of K. A proof of Theorem 1 with explicit calculation of a possible t_K (in terms of simple geometric characteristics of K) will be given in Section 3. It is based on elementary convexity arguments. Before we discuss computational issues in the next section, it is worth to mention an application of Theorem 1 to random sets. The most common model for a random set is the so-called *Boolean model Z with convex particles*. Roughly speaking, it is obtained by attaching independent identically distributed particles in $\mathcal{K}$ to random points in the plane that have a homogeneous Poisson property. Molchanov [14] devotes a monograph to the Boolean model. Estimation of the (specific) Euler characteristic of Boolean models from digitizations has been a subject of interest since Serra's results [6] on this matter. The observation $Z \cap W$ of Z in a test window $W \in \mathcal{K}$ is random set with $Z \cap W \in \mathcal{R}$ almost surely. If the particles of Z and W are in addition full dimensional, then $Z \cap W \in \tilde{\mathcal{R}}$ holds almost surely. Theorem 1 can therefore be applied: Almost surely, there is a constant $t(Z \cap W) > 0$ such that the Euler characteristic of $Z \cap W$ is estimated correctly from $Z \cap t\mathbb{L}$ in W by the new estimator of χ, whenever $t < t(Z \cap W)$. Extensions and a comparison of this result with earlier results on the digitization of Boolean models are planned in the follow-up paper [15].

2 Computional issues

The approaches in a), b) and c) have the computational advantage that the estimators can be calculated locally. This means that only the occurrence of small pixel configurations must be counted and the estimator is then obtained as a weighted sum of these numbers. To describe this in detail, let $\mathbb{L} = \mathbb{Z}^2$ be the standard lattice and $t = 1$. We introduce an intuitive notation for *configurations*, where lattice points in K are thought of to be black. For instance, the configuration $\begin{bmatrix} \circ & \cdot \\ \bullet & \circ \end{bmatrix}$ indicates that four fixed points in a 2×2-block of the lattice do not hit K in the lower right and upper left corner, but they hit K in the lower left. The behaviour of the remaining corner is not specified. Let $\# \begin{bmatrix} \bullet & \cdot \\ \circ & \bullet \end{bmatrix}$ the number of occurrences of this configuration in the digital image $K \cap \mathbb{Z}^2$. Using Euler's formula for graphs in a) and c) and the additivity of χ in b), it follows that the estimator $\hat{\chi}$ of the Euler characteristic satisfies

$$\hat{\chi} = \# \begin{bmatrix} \circ & \cdot \\ \bullet & \circ \end{bmatrix} - \# \begin{bmatrix} \bullet & \circ \\ \bullet & \bullet \end{bmatrix} \tag{7}$$

for a) with the 4-neighbourhood and b) with $\mathcal{P}_4$, and

$$\hat{\chi} = \# \begin{bmatrix} \circ & \circ \\ \bullet & \circ \end{bmatrix} - \# \begin{bmatrix} \bullet & \circ \\ \bullet & \bullet \end{bmatrix}$$

for a) with the 6-neighbourhood and for c); cf. Ohser & Mücklich [16] and Serra [6]. For a) with the 8-neighbourhood and b) with $\mathcal{P}_8$, we have

$$\hat{\chi} = \# \begin{bmatrix} \circ & \bullet \\ \circ & \circ \end{bmatrix} - \# \begin{bmatrix} \bullet & \cdot \\ \circ & \bullet \end{bmatrix}.$$

Up to a rotation with 180 degrees (which leaves χ and $\hat{\chi}$ unchanged) we therefore obtain the dual version of (7): black and white points are interchanged and the sign is reversed. This is in accordance with the planar consistency relation

$$\chi(K) = -\chi(K^C).$$

Up to now we have interpreted the digital picture of K as the set of lattice points in K. In applications, this picture is actually an array of black and white points in a rectangular window W. We may assume that the boundary of W does not hit K to avoid edge-effects. If N denotes the number of lattice points in W, (7) and its variants show that all the estimators in a), b) and c) can be calculated in one scan of the image, hence with $O(N)$ operations. Implementations use evaluation of the image with varying filter masks, see e.g. Ohser & Mücklich [16, p. 137]. The recursive algorithm of Bieri & Nef [17], descending in dimension, depends on the complexity of K, rather than on N. It is in general faster than naive approaches; its worst case behaviour is also $O(N)$. Dyer [18] developed an algorithm to determine $\hat{\chi}$ using quadtrees. Clearly (7) and its variants only involve boundary lattice points (lattice points in K with at least one neighbour in K^C). Lee *et al.* [11] notice that the complexity can therefore be reduced to $O(n)$, where n is the number of boundary lattice points. This is relevant, if a list of these points is needed anyway to determine other characteristics of the image.

To calculate the new estimator, the numbers of connected components of $\hat{P} = \hat{P}_1$ and $\hat{Q} = \hat{Q}_1$ with interior points must be determined. This can be done simultaneously with common region detecting algorithms. For example, the Rosenfeld-Pfaltz labeling algorithm [19] can be modified to yield these numbers: In a first scan, this algorithm labels the points of the image in a sequential manner either with an already existing label of an 8-neighbour, or with a new label, if none of the neighbours is labeled. At the same time, a table of equivalent labels is recorded. In a second scan, each label is replaced by a representative in its equivalence class. This algorithm is modified as follows: During the first scan it is decided whether the current pixel belongs to a 2×2-block of the lattice with all colors equal. As this is a local property, the test can be included in the algorithm without extra costs. We then introduce an additional mark in the equivalence table identifying those labels, whose connected component contains an interior point. The second scan is not necessary any more, as we are only interested in the *number* of connected components. This shows that the complexity of the modified algorithm is one scan of the image plus the costs of a standard transversal algorithm to find all equivalent labels in the equivalence table. The costs of the latter can not be larger than the costs of one scan of the original image.

Summarizing, the new algorithm is not more than twice as time consuming than the common estimators for χ. But besides the fact that it also yields the number of connected components and the number of holes, it has the advantage that it yields the correct result for sufficient high resolution of the image, provided that $K \in \tilde{R}$. The new estimator therefore is geometrically more stable at the cost of a rather small increase in calculation time.

3 Proofs

For $A \subset \mathbb{R}^2$, we introduce the notations $\operatorname{int} A$, ∂A and $\operatorname{cl} A$ for the topological interior, boundary and closure of A, respectively. Let $\alpha A = \{\alpha a \mid a \in A\}$ be the scaling of A with $\alpha \in \mathbb{R}$. For negative α, this includes a central reflection at the origin o. The *Minkowski-sum* of two sets $A, B \subset \mathbb{R}^2$ is given by

$$A \oplus B = \{a + b \mid a \in A, b \in B\}$$

and if one is a singleton, we write $a + B = \{a\} \oplus B$ and $A + b = A \oplus \{b\}$ for the corresponding translations. Their *Minkowski-difference* is given by

$$A \ominus B = \bigcap_{b \in B} (A + b)$$

and the *morphological opening of A with B* by

$$A \circ B = (A \ominus B) \oplus B.$$

The Euclidean norm of $x \in \mathbb{R}^2$ is denoted by $\|x\|$, the unit disk by $B^2 = \{x \in \mathbb{R}^2 \mid \|x\| \leqslant 1\}$ and the unit circle by $S^1 = \partial B^2$. The line through the origin with normal $u \in S^1$ is denoted by $u^\perp$. The *support cone* of a convex body K at $x \in K$ is defined by

$$S(K, x) = \operatorname{cl} \bigcup_{\lambda \geqslant 0} \lambda(K - x).$$

We refer the reader to Schneider [20] for further notions and definitions from convex geometry. The required basic graph theoretic notions can be found in any introductory textbook on the matter, e.g. in West's book [21].

To show that $\hat{N}_c(\hat{P}_t)$ equals $N_c(K)$ for sufficiently small t, four preparatory lemmas are proven. We start with a lemma which shows that any set $K \in \tilde{\mathcal{R}}$ can locally be written as union of at most two convex sets.

Lemma 2 *For any $K \in \tilde{\mathcal{R}}$ there is an $\varepsilon > 0$ such that for all $z \in \mathbb{R}^2$ there are $i_1, i_2 \in \{1, \ldots, m\}$ with*

$$(z + \varepsilon B^2) \cap K = (z + \varepsilon B^2) \cap (K_{i_1} \cup K_{i_2}). \qquad (8)$$

PROOF. Let $K = \bigcup_{i=1}^m K_i$, $K_i \in \mathcal{K}$, be a representation of K satisfying the conditions (i) and (ii) in Definition 1. Let $S = \{\partial K_i \cap \partial K_j \mid 1 \leqslant i < j \leqslant m\}$. We show (8) first for all $z = p \in S$: there is $\delta > 0$ such that for all $p \in S$

$$\text{there are } i_1, i_2 \in \{1, \ldots, m\} : (p + \delta B^2) \cap K = (p + \delta B^2) \cap (K_{i_1} \cup K_{i_2}). \qquad (9)$$

As S is assumed to be finite, we may fix $p \in S$ and show (9) for this p. If $p \in \operatorname{int} K_i$ for some i, the claim is obvious and we assume $p \notin \bigcup_{i=1}^m \operatorname{int} K_i$. Let $k \geqslant 1$ be the number of sets in $\{K_1, \ldots, K_m\}$ whose boundary contains p; without loss of generality let

$p \in \partial K_1 \cap \ldots \cap \partial K_k$ and $p \notin K_i$ for $i > k$. The intersection-regularity of K implies that there is a $\tau > 0$ and $y \in \mathbb{R}^2$, $y \neq p$, such that $y + \tau B^2 \subset K_1 \cap \ldots \cap K_k$. Let $g = \{p + \alpha(y - p) \mid \alpha \in \mathbb{R}\}$ be the line through p and y. The half-open ray $\{p + \alpha(y - p) \mid \alpha < 0\}$ does not hit any of the sets $K_1 \ldots K_k$, as otherwise p would be an interior point of the corresponding K_i by convexity. Let H^+ be one of the open half planes bounded by g. We claim that there is an $i \in \{1, \ldots, k\}$ such that for sufficiently small $\delta > 0$, we have

$$(p + \delta B^2) \cap K \cap H^+ = (p + \delta B^2) \cap K_i \cap H^+. \tag{10}$$

Repetition of the same arguments for the other open half plane $H^- = \mathbb{R}^2 \setminus (H^+ \cup g)$ then shows that (9) is true. We prove (10). Without loss of generality assume that p is the origin, g is the x-axis and y is a point with negative x-value. Without loss of generality, let K_1 be the convex body in the set $\{K_1, \ldots, K_k\}$ whose boundary, intersected with H^+, (a convex curve through $p = o$) has the smallest slope in o. As ∂K_i, $i \neq 1$, hits ∂K_1 only in finitely many points, $H^+ \cap \partial K_i \cap (p + \delta' B^2)$, $i \neq 1$, hits ∂K_1 only in p for some suitably small $\delta' > 0$. Hence there is an $\delta > 0$ such that $\text{conv}\{y, \partial K_1 \cap (p + \delta' B^2) \cap H^+\}$ contains all sets $H^+ \cap K_i \cap (p + \delta B^2)$. This shows (10) with $i = 1$.

We now use (9) to show (8). Assume that $\delta > 0$ is chosen such that (9) holds for all $p \in S$ and consider the family of all connected components of the sets $\partial K_j \setminus \bigcup_{p \in S}(\text{int}(p + \delta/3B^2)), j = 1, \ldots, m$. The members of this finite family are disjoint compact convex arcs. Thus there is a $0 < \varepsilon < \delta/3$ with the property that any disk $z + \varepsilon B^2$ either hits $p + \delta/3B^2$ for some $p \in S$, or it hits at most one of the boundaries $\partial K_1, \ldots, \partial K_m$. In the first case we have $z + \varepsilon B^2 \subset p + \delta B^2$ and thus (8) holds. In the second case we may assume without loss of generality that $z + \varepsilon B^2$ does not hit $\partial K_2, \ldots, \partial K_m$. If $z + \varepsilon B^2$ does not hit any of the sets $K_2, \ldots, K_m$, then (8) holds; otherwise $z + \varepsilon B^2$ must be completely contained in some K_j, $j = 2, \ldots, m$, as $\partial K_j \cap (z + \varepsilon B^2) = \emptyset$. Again this implies (8) and the proof is complete.

We define some constants, which will be useful in the sequel.

Definition 2 *Let a nonempty set $K \in \tilde{\mathcal{R}}$ be given and $K = \bigcup_{i=1}^m K_i$ be a representation satisfying the conditions (i) and (ii) in Definition 1.*

(1) Let $t_0 = t_0(K_1, \ldots, K_m)$ be the supremum of all ε such that (8) *holds (where $t_0 = \infty$ is allowed and occurs in particular for $m \leqslant 2$).*
(2) Let $t_1 = t_1(K_1, \ldots, K_m)$ be the largest positive number such that for any $\emptyset \neq I \subset \{1, \ldots, m\}$ with $\bigcap_{i \in I} K_i \neq \emptyset$, there is a ball of radius $2t_1$ contained in this intersection.
(3) Let $t_2 = t_2(K_1, \ldots, K_m) > 0$ be the supremum of all $r > 0$ such that for any $\emptyset \neq I \subset \{1, \ldots, m\}$ with $\bigcap_{i \in I} K_i = \emptyset$, the set $\bigcap_{i \in I}(K_i \oplus rB^2)$ is empty. (Again, $t_2 = \infty$ may occur.)

We discuss some consequences of these definitions. Let $\mathbb{L}$ be a regular lattice generated by the basis x_1, x_2 of $\mathbb{R}^2$ and let C_0 be the corresponding closed unit cell. Any lattice translation $x + \mathsf{C}_0$, $x \in \mathbb{L}$, of the closed unit cell will be called a *cell of* $\mathbb{L}$. Assume $\|x_i\| \leqslant 1$ for $i = 1, 2$. Consider Definition 2.(2) and fix an index set I with $\bigcap_{i\in I} K_i \neq \emptyset$. If $t \leqslant t_1$, there is a ball $z + 2tB^2$ contained in this intersection. As the union of all scaled cells $t(x + \mathsf{C}_0)$, $x \in \mathbb{L}$, is $\mathbb{R}^2$, there is a scaled cell C containing z. The diameter of C is less than $2t$, so

$$C \subset z + 2tB^2 \subset \bigcup_{i\in I} K_i.$$

Hence, $t \leqslant t_1$ implies that every nonempty intersection contains a cell of $t\mathbb{L}$. If $t < t_2$ and I is as in Definition 2.(3), then for all $x \in \mathbb{L}$ and $F \in \mathcal{P}_0$, there must be an $i \in I$ with $t(x + F) \cap K_i = \emptyset$.

The constants t_0, t_1 and t_2 not only depend on K, but on a representation of K satisfying the conditions (i) and (ii) in Definition 1. In the following, we will not make this dependence explicit. Whenever these constants are used, they are meant with respect to a fixed underlying representation of $K \in \tilde{\mathcal{R}}$.

Fix $K \in \mathcal{R}$ and let $\hat{P}_t$ be given by (5). Recall that the 8-connected graph $\mathcal{G}_8(K)$ has vertex set $K \cap \mathbb{L}$ and its undirected edges are of the form $\{a, b\}$, with $a, b \in K \cap \mathbb{L}$ and $a - b \in \{\pm x_1, \pm x_2, \pm(x_1 + x_2), \pm(x_1 - x_2)\}$. If, for instance, $\mathbb{L} = \mathbb{Z}^2$ with closed unit cell $[0, 1]^2$, then the family of edges is

$$\Big\{\{a, b\} \mid a, b \in K \cap \mathbb{Z}^2 \text{ and } 0 < \|a - b\| \leqslant \sqrt{2}\Big\}.$$

Two points $a, b \in K \cap \mathbb{L}$ belong to the same connected component of $\hat{P}_t$ if and only if there is an edge path in $\mathcal{G}_8(K)$ from a to b. To show connectivity properties of $\hat{P}_t$ it is therefore sufficient to construct suitable paths in $\mathcal{G}_8(K)$. The next lemma restricts considerations to convex bodies K. It implies that $\hat{N}_c(\hat{P}_t)$ yields the correct result $\chi(K) = 1$, if K contains at least one cell of $t\mathbb{L}$.

Lemma 3 *Let K be a convex body, $\mathbb{L}$ a lattice with closed unit cell C_0 and let $C = x + \mathsf{C}_0, x \in \mathbb{L}$, and $\tilde{C} = \tilde{x} + \mathsf{C}_0, \tilde{x} \in \mathbb{L}$, be two cells. If $C \subset K$ and at least three of the vertices of $\tilde{C}$ are in K, then there is an edge path from a vertex of C to a vertex of $\tilde{C}$ in $\mathcal{G}_8(K)$.*

PROOF. Let V be the set of vertices of $\tilde{C}$ in K. By convexity, K contains $\mathrm{conv}(C \cup V)$, and we may assume without loss of generality that $K = \mathrm{conv}(C \cup V)$. Applying a suitable affine transform, we may further assume that $\mathbb{L} = \mathbb{Z}^d$, that $C = [0, 1]^2$ and that V is contained in the closed first quadrant Q_+.

Let Γ be the set of all paths $\gamma = (z_0, \ldots, z_s)$ in $\mathcal{G}_8(K)$ with the following properties:
(1) γ starts in $z_0 = (1, 1)$,
(2) for all $n = 1, \ldots, s$, we have $z_n \in z_{n-1} + Q_+$, i.e. the n-th edge $\{z_{n-1}, z_n\}$ increases the x-value or the y-value (or both) when walking from z_{n-1} to z_n.

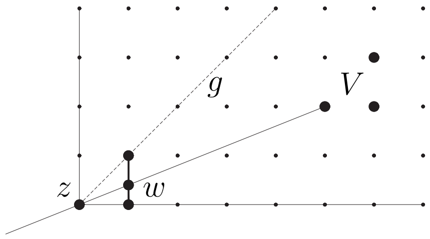

Fig. 3. Construction of a longer path from the endpoint z of γ_0; see text.

(3) the endpoint $z = z_s$ of γ satisfies $V \subset z + Q_+$, so x- and y-values of the endpoint are not larger than x- and y-values of the elements of V.

Let γ_0 be a path with maximal length in Γ. If there was no path in $\mathcal{G}_8(K)$ connecting a vertex of C with an element of V, then the endpoint z of γ_0 would not be an element of V. By construction, $C \subset z + (-Q_+)$ and $V \subset z + Q_+$. Denote the bisecting line of $z + Q_+$ by g and assume without loss of generality that V has at least one point below g (this possibly requires a reflection at g). As $z \in K = \operatorname{conv}(C \cup V)$ and $C \subset z + (-Q_+)$, the line segment $e = [z + (1, 0), z + (1, 1)]$ must hit K in a point w, see Figure 3. V consists of three or four vertices of a cell and thus, $\operatorname{conv} V$ contains a vertical line of length 1. This is obviously also true for C. Thus, the intersection of $K = \operatorname{conv}(C \cup V)$ with the horizontal line through w has length at least 1 and therefore at least one of the vertices of e is in K. Call this vertex z'; if both vertices of e are in K, then choose the lower, $z' = z + (1, 0)$. The path γ_0 can prolonged with the additional edge $\{z, z'\}$ contradicting the maximal length of γ_0.

We note the following corollary, where the set

$$\operatorname{clip}(K, t) = (K \circ t[-x_1, x_1]) \cap (K \circ t[-x_2, x_2])$$

for $K \in \mathcal{K}$ is used. It depends on $t \geqslant 0$ and on two vectors $x_1, x_2 \in \mathbb{R}^2$. The latter dependence is not made explicit in the notation; in what follows x_1, x_2 are always given by the context, as they are vectors which generate the lattice $\mathbb{L}$. If $(2x_1, 2x_2)$ is the standard basis, K has a smooth boundary and t is small enough, then $\operatorname{clip}(K, t)$ is obtained from K by cutting off two vertical and two horizontal strips such that the length of the linear cutting lines are t. Note that a point $x \in K$ is in $\operatorname{clip}(K, t)$ if and only if for $i = 1, 2$, the line through x with direction x_i hits K in a line segments of length $2t$ or more.

Corollary 4 *Let K be a convex body, $\mathbb{L}$ a lattice generated by x_1, x_2 with $\|x_1\| \leqslant 1, \|x_2\| \leqslant 1$. If the cell $C = x + \mathsf{C}_0, x \in \mathbb{L}$, is contained in K and*

$$v \in \mathbb{L} \cap \operatorname{clip}(K, 1),$$

then there is an edge path from v to a vertex of C in the graph $\mathcal{G}_8(K)$.

PROOF. Let the assumptions be satisfied. As $v \in \mathbb{L} \cap \operatorname{clip}(K, 1)$, one of the lattice points $v + x_1$ or $v - x_1$ must be in K. Similarly, one of the lattice points $v + x_2$ or

$v - x_2$ is in K and thus there is a cell $\tilde{C} = \tilde{x} + \mathsf{C}_0$ with three vertices in K, v being one of them. The claim now follows from Lemma 3.

In the next two lemmas, pairs of convex bodies are considered.

Lemma 5 *Let K_1 and K_2 be two convex bodies with $\operatorname{int}(K_1 \cap K_2) \neq \emptyset$ and such that $\partial K_1 \cap \partial K_2$ is finite. Let $\mathbb{L}$ be a lattice generated by x_1, x_2 with closed unit cell C_0. Then there is an $\varepsilon = \varepsilon(K_1, K_2, x_1, x_2) > 0$ such that for all $0 < t \leqslant \varepsilon$, we have:*

If $C = t(x + \mathsf{C}_0)$, $x \in \mathbb{L}$, is a scaled cell with vertices in $K_1 \cup K_2$, then one of the following holds:

(1) $\operatorname{conv}\Big((K_1 \cap K_2) \cup C\Big) \subset K_1 \cup K_2$,
(2) $\operatorname{vert} C \cap \operatorname{clip}(K_1, t) \neq \emptyset$ *or* $\operatorname{vert} C \cap \operatorname{clip}(K_2, t) \neq \emptyset$.

Condition *(1)* is equivalent to the statement $C \subset K_1 \cup K_2$, but the formulation in *(1)* is more convenient for later use.

PROOF. For $p \in \partial K_1 \cap \partial K_2$ and $i = 1, 2$ let $\alpha_i(p)$ be the shorter length of the line segments $K_i \cap \{p + \beta x_j \mid \beta \in \mathbb{R}\}$, $j = 1, 2$. As $\partial K_1 \cap \partial K_2$ is finite, the number

$$\alpha = \min_{i=1,2} \min \{\alpha_i(p) \mid p \in \partial K_1 \cap \partial K_2 \text{ such that } \alpha_i(p) > 0\}$$

is positive. We have $p \in \operatorname{clip}(K_i, \alpha)$ for all p with $\alpha_1(p) > 0$ or $\alpha_2(p) > 0$. By convexity of K_i there is a $\delta_i > 0$ with the following property: if $v \in K_i$ satisfies $\|v - p\| \leqslant \delta_i$ for some $p \in \partial K_1 \cap \partial K_2$ with $\alpha_i(p) > 0$, then $v \in \operatorname{clip}(K_i, \alpha/2)$. Put $\delta = \min\{\delta_1, \delta_2\}$ and

$$\varepsilon = \min \left\{ \frac{\alpha}{2}, \frac{2t_1}{D}\delta \right\}, \tag{11}$$

where $t_1 = t_1(K_1, K_2)$ is given by Definition 2.(2) and D is the diameter of $K_1 \cap K_2$. Now let $0 < t \leqslant \varepsilon$ and a scaled cell $C = t(x + \mathsf{C}_0)$, $x \in \mathbb{L}$, with vertices in $K = K_1 \cup K_2$ be given and consider the following cases.

1st Case: All four edges of the cell C are contained in K. Let e be one of the edges of C. Then, by the convexity of K_1 and K_2, any segment $[y, z]$ with $y \in e$ and $z \in K_1 \cap K_2$ is contained in K_1 or in K_2. Hence $[y, z] \subset K$. As $K_1 \cap K_2$ and e are convex, we obtain $\operatorname{conv}\Big((K_1 \cap K_2) \cup e\Big) \subset K$. As e was arbitrary among the four edges of C, and $K_1 \cap K_2$ is non-empty, this implies (1).

2nd Case: There is an edge $[v_1, v_2]$ of C not contained in K. We may assume without loss of generality that $v_1 \in K_1$ and $v_2 \in K_2$. From (11), we get

$$\|v_1 - v_2\| \leqslant t \leqslant \varepsilon \leqslant \frac{2t_1}{D}\delta.$$

Application of Lemma 6, below, yields the existence of a $p \in \partial K_1 \cap \partial K_2$ such that

$$\max_{i=1,2} \|p - v_i\| \leqslant \delta. \tag{12}$$

We will now show that $\alpha_1(p) > 0$ or $\alpha_2(p) > 0$. Without loss of generality, we may assume that the line through v_1 and v_2 has direction x_1. The parallel line through p is $\{p + \beta x_1 \mid \beta \in \mathbb{R}\}$. By Lemma 6.(3) and $\mathrm{int}(K_1 \cap K_2) \neq \emptyset$, this line hits $\mathrm{conv}((K_1 \cap K_2) \cup \{v_i\})$, and hence K_i, in a non-degenerate line segment. Now consider the line $h = \{p + \alpha x_2 \mid \alpha \in \mathbb{R}\}$. We will show that either K_1 or K_2 hits h in a non-degenerate line segment. Otherwise $h \cap K = \{p\}$ and Lemma 6.(2) would imply that v_1 and v_2 are on different sides of h. Therefore, choosing an arbitrary disk $B = z + \tau B^2 \subset K_1 \cap K_2$, $\tau > 0$, either $\mathrm{conv}(B \cup \{v_1\}) \subset K_1$ or $\mathrm{conv}(B \cup \{v_2\}) \subset K_2$ hits h in a line segment of positive length. Hence K_1 or K_2 has a non-degenerate intersection with h. Summarizing, we have $p \in \partial K_1 \cap \partial K_2$ and for at least one $i \in \{1, 2\}$ the variable $\alpha_i(p)$ is positive. The latter implies $p \in \mathrm{clip}(K_i, \alpha)$. Thus $v_i \in \mathrm{clip}(K_i, \alpha/2)$ due to (12). In view of $t \leqslant \varepsilon \leqslant \alpha/2$, this gives the second case in the statement of the lemma.

Lemma 6 *Let K be the union of the two convex bodies K_1 and K_2 with* $\mathrm{int}(K_1 \cap K_2) \neq \emptyset$. *Let D be the diameter of $K_1 \cap K_2$. Then for all $\varepsilon > 0$ and $v_1 \in K_1$, $v_2 \in K_2$ with*

$$[v_1, v_2] \not\subset K \quad \textit{and} \quad \|v_1 - v_2\| \leqslant \frac{2t_1}{D}\varepsilon,$$

there is a $p \in \partial K_1 \cap \partial K_2$ with the following properties:

(1) $\|v_1 - p\| \leqslant \varepsilon$, $\|v_2 - p\| \leqslant \varepsilon$,
(2) any closed ray $\tilde{R}$ emanating from p with $\tilde{R} \cap K = \{p\}$ and hitting the line g through v_1 and v_2, hits $[v_1, v_2]$.
(3) the parallel of g through p separates $K_1 \cap K_2$ and $[v_1, v_2]$.

PROOF.

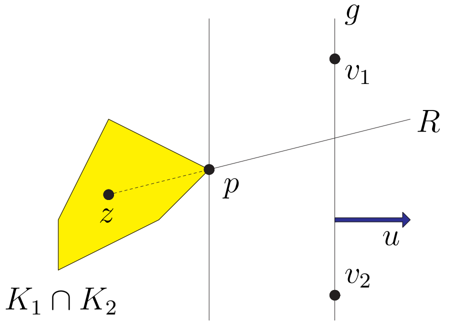

Fig. 4. The construction of $p \in \partial K_1 \cap \partial K_2$ and the ray R.

Let $[v_1, v_2] \not\subset K_1 \cup K_2$ be given with $v_1 \in K_1$, $v_2 \in K_2$ and $\|v_1 - v_2\| \leqslant 2t_1\varepsilon/D$. v_1 and v_2 cannot be members of the same K_i, so $v_1 \in K_1 \setminus K_2$ and $v_2 \in K_2 \setminus K_1$. The line g through v_1 and v_2 cannot hit the convex set $K_1 \cap K_2$, so there is a unit vector u such that $g = v_1 + u^\perp$ and $K_1 \cap K_2 \subset \{\langle \cdot, u \rangle < \langle v_1, u \rangle\}$; see Figure 4. Let p be a support point of $K_1 \cap K_2$ with outer unit normal u. Clearly, $p + u^\perp$ separates $K_1 \cap K_2$ and g, so (3) holds. For $z \in \mathrm{int}(K_1 \cap K_2)$, the relative open ray $R = \{p - \alpha(z-p) \mid \alpha > 0\}$ cannot contain any points of K and thus $p \in \partial K_1 \cap \partial K_2$. In Figure 4, the points v_1 and v_2 lie on different sides of R. This is necessarily so and follows from claim (2), which will be shown at the end of this proof.

Let

$$S_p = -S(K_1 \cap K_2, p) + p$$

be the reflected and translated support cone of $K_1 \cap K_2$ at p. As we have used an arbitrary $z \in \mathrm{int}(K_1 \cap K_2)$ to define R, we may conclude that S_p is contained in the convex cone

$$p + \bigcup_{\lambda \geqslant 0} \lambda([v_1, v_1] - p).$$

The opening angle of the latter cone is therefore larger than the one of the support cone, which is bounded from below by $\varphi = 2 \arcsin(2t_1/D)$. The distance between v_1 and v_2 is at most $\beta = 2t_1\varepsilon/D$. For $\varphi \geqslant \pi/2$, this implies

$$\max_{i=1,2} \|p - v_i\| \leqslant \beta < \varepsilon,$$

as $2t_1/D \leqslant 1/2$. For $\varphi \leqslant \pi/2$, elementary geometry implies

$$\max_{i=1,2} \|p - v_i\| \leqslant \frac{\beta}{\sin\varphi} \leqslant \frac{\beta}{\sin\varphi/2} = \varepsilon.$$

This is gives (1).

It remains to show claim (2). We assume that there is a closed ray $\tilde{R}$ such that (2) is violated, which means that v_1 and v_2 are on the same side of the line spanned by $\tilde{R}$. To fix ideas, we again consider the geometry in Figure 4, and assume without loss of generality that v_1 is between v_2 and the intersection of $\tilde{R}$ with g. Consider an arbitrary $z \in K_1 \cap K_2$ and let h' be the line through p and v_1. If z was in the open half plane bounded by h' not containing v_2, then $[z, v_1] \subset K_1$ would hit $\tilde{R}$, and $\tilde{R}$ would contain a point of K other than p, which contradicts the assumptions. If, however z was in the other open half space bounded by h', the intersection of $[z, v_1] \subset K_1$ with $[p, v_2] \subset K_2$ would contain a point q with $\langle p, u\rangle < \langle q, u\rangle$, which contradicts the definition of p. As z was arbitrary in $K_1 \cap K_2$, we conclude $K_1 \cap K_2 \subset h'$. This gives the final contradiction $\mathrm{int}(K_1 \cap K_2) = \emptyset$.

Definition 3 *Let $K \in \tilde{\mathcal{R}}$ be given and $K = \bigcup_{i=1}^m K_i$ be a representation satisfying the conditions (i) and (ii) in Definition 1. Let, in addition, a basis x_1, x_2 of $\mathbb{R}^2$ be given.*

(1) For any two different indices $i_1, i_2 \in \{1, \ldots, m\}$ there is an $\varepsilon = \varepsilon(K_{i_1}, K_{i_2}, x_1, x_2) > 0$ such that Lemma 5 holds with K_{i_1}, K_{i_2} replacing K_1 and K_2, respectively. Define $t_3 = t_3(K_1, \ldots, K_m, x_1, x_2)$ by

$$t_3 = \min_{i_1 \neq i_2 \in \{1,\ldots,m\}} \varepsilon(K_{i_1}, K_{i_2}, x_1, x_2).$$

(2) For any two different indices $i_1, i_2 \in \{1, \ldots, m\}$ let $D(K_{i_1}, K_{i_2})$ be the diameter of $K_{i_1} \cap K_{i_2}$ and define $t_4 = t_4(K_1, \ldots, K_m)$ by

$$t_4 = \min_{i_1 \neq i_2 \in \{1,\ldots,m\}} \frac{2t_1(K_{i_1}, K_{i_2})}{D(K_{i_1}, K_{i_2})}.$$

Note that only t_3 depends on the basis. The constant t_4 is independent of scaling:

$$t_4(tK_1, \ldots, tK_m) = t_4(K_1, \ldots, K_m)$$

holds for all $t > 0$. Furthermore

$$t_4 \leqslant \tfrac{1}{2}, \tag{13}$$

as the diameter of a set containing a ball of radius $2t_1$ is at least $4t_1$. The multigrid convergence of the estimator $\hat{N}_c(\hat{P}_t)$ can now be stated.

Theorem 7 *Let $K \in \tilde{\mathcal{R}}$ be given and let $\mathbb{L}$ be a lattice generated by a basis x_1, x_2 of $\mathbb{R}^2$ with $\|x_1\| \leqslant 1,\ \|x_2\| \leqslant 1$. Then*

$$\hat{N}_c(\hat{P}_t) = N_c(K)$$

for all $0 < t < \min\{t_0, t_1, t_2, t_3\}$.

PROOF. Let $k \in \mathbb{N}$ be the number of connected components of K. (Applying possibly a shift of indices) assume that the connected component M_j contains the convex body K_j, $j = 1, \ldots, k$. To simplify notation further, assume that $t < \min\{t_0, t_1, t_2, t_3\}$ is equal to 1.

Due to $1 = t < t_1$, there is a cell $C_j = x_j + \mathsf{C}_0$, $x_j \in \mathbb{L}$, in $K_j \subset M_j$ for each $j = 1, \ldots, k$. The cells $C_1, \ldots, C_k$ are subsets of $\hat{P}_1$. Fix C_j with $1 \leqslant j \leqslant k$ and some other cell $\tilde{C} = x + \mathsf{C}_0 \subset \hat{P}_1$, $x \in \mathbb{L}$. We show that these two cells belong to the same connected component of $\hat{P}_1$ if and only if their vertices all are in the same connected component of K. Applying this with $\tilde{C} = C_l, l = 1, \ldots, k$ will yield $\hat{N}_c(\hat{P}_1) \geqslant k = N_c(K)$ and with $\tilde{C}$ being any other cell in $\hat{P}_1$ will give $\hat{N}_c(\hat{P}_1) \leqslant k = N_c(K)$. The Theorem thus follows from this new claim.

If C_j and $\tilde{C}$ are in the same connected component of $\hat{P}_1$, then there is an edge-path in $\mathcal{G}_8(K)$ of line segments connecting vertices of the two cells. If $\operatorname{vert} C_j \cup \operatorname{vert} \tilde{C}$ would not be a subset of one connected component of K, there would be a first edge in this edge-path with starting point in one connected component and endpoint in another. But $1 = t < t_2$ states that this is impossible. Thus $\operatorname{vert} C_j$ and $\operatorname{vert} \tilde{C}$ are in the same connected component of K.

Assume now that $\operatorname{vert} C_j \cup \operatorname{vert} \tilde{C} \subset M_j$ for a connected component M_j of K. The cell C_j is completely contained in $K_j \subset M_j$. By $\tilde{C} \subset \hat{P}_1$, $1 = t < t_0$ and Lemma 2 we have

$$\operatorname{vert} \tilde{C} = (\operatorname{vert} \tilde{C}) \cap K = (\operatorname{vert} \tilde{C}) \cap (K_{i_1} \cup K_{i_2}) \subset K_{i_1} \cup K_{i_2} \tag{14}$$

for some suitable $i_1, i_2 \in \{1, \ldots, m\}$. By $1 = t < t_1$, the set $K_{i_1} \cap K_{i_2}$ contains a cell $C_{1,2} = x + \mathsf{C}_0$, $x \in \mathbb{L}$. As $\tilde{C}$ hits the component M_j, the sets K_{i_1} and K_{i_2} must hit M_j, as well, and the cells $C_j, \tilde{C}$ and $C_{1,2}$ all hit M_j. As C_j and $C_{1,2}$ hit the same connected component of K, there is a chain of sets

$$K_j = K_{j_1}, K_{j_2}, \ldots, K_{j_{n-1}}, K_{j_n} = K_{i_1}$$

where any two consecutive sets have a nonempty intersection; see Figure 5.

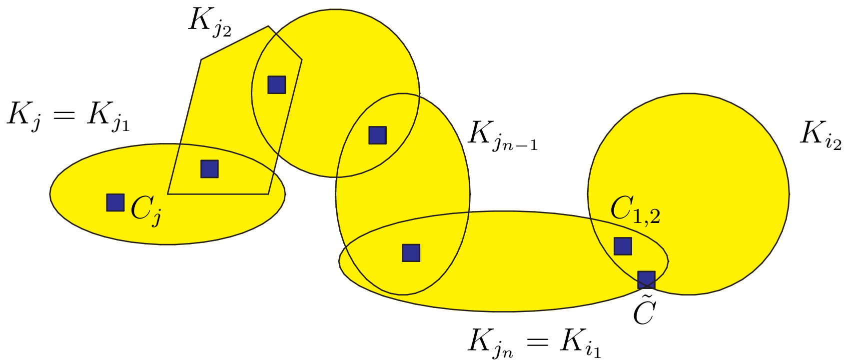

Fig. 5. The chain of sets connecting C_j, $C_{1,2}$ and $\tilde{C}$.

Any of these intersections contains a cell $x + \mathsf{C}_0$, $x \in \mathbb{L}$, and repeated application of Lemma 3 yields an edge path in $\mathcal{G}_8(K)$ starting in a vertex of C_j, passing all these cells and ending in a vertex of $C_{1,2}$. In view of (14) and $1 = t < t_3$, Lemma 5 with K_1, K_2 replaced by K_{i_1}, K_{i_2}, respectively, shows that either

$$\operatorname{conv}(C_{1,2} \cup \tilde{C}) \subset \operatorname{conv}((K_{i_1} \cap K_{i_2}) \cup \tilde{C}) \subset K_{i_1} \cup K_{i_2} \subset K, \qquad (15)$$

or that $\tilde{C}$ has a vertex in $\operatorname{clip}(K_{i_1}, t)$ or in $\operatorname{clip}(K_{i_2}, t)$. If (15) holds, Lemma 3 can be applied to the convex body $\operatorname{conv}(C_{1,2} \cup \tilde{C})$ to find a path in $\mathcal{G}_8(K)$ connecting $C_{1,2}$ and $\tilde{C}$. Otherwise, the existence of such a path follows from Corollary 4. Putting things together, we have constructed a path in $\mathcal{G}_8(K)$ connecting C_j and $\tilde{C}$ (passing $C_{1,2}$) and thus, C_j and $\tilde{C}$ are contained in the same connected component of $\hat{P}_1$. This completes the proof.

We now treat the number of holes $N_h(\cdot)$ of a set $K \in \tilde{\mathcal{R}}$. Note that the arguments for $N_c(\cdot)$ cannot be used directly, as the class $\tilde{\mathcal{R}}$ is not closed under the operation of set-complements. We first prove two lemmas, the first of which states that the minimal distance of connected components of K^C is bounded from below by a constant already defined.

Lemma 8 *Let $K \in \tilde{\mathcal{R}}$ be given. Then the distance between two different connected components of K^C is at least $4t_1$.*

PROOF. Let $K = \bigcup_{i=1}^m K_i, K_i \in \mathcal{K}$, be given and assume that the statement is wrong. Then there are two points d and d' in different connected components of K^C

such that the line segment $[d, d']$ has length less than $4t_1$. Without loss of generality, we may assume that $[d, d'] \cap K$ is a line segment, as otherwise we can choose points on $[d, d']$ with the same properties but even smaller distance. Let D and D' be the connected components of K^C containing d and d', respectively. By suitable indexing, we may assume that all the convex bodies $K_1, \dots, K_k$ hit $[d, d']$, whereas none of $K_{k+1}, \dots, K_m$ does. The set K_1 contains a disk $z_1 + 2t_1 B^2$ with midpoint $z_1 \in \mathbb{R}^2$. As $d, d' \in K^C$ and the length of $[d, d']$ is less than $4t_1$, z_1 cannot be an element of the line g spanned by $[d, d']$. Let H be the closed half plane bounded by g and not containing z_1. We proceed by proving the following steps:

Step (1): None of the sets $K_1, \dots, K_k$ contains a disk of radius $2t_1$ with midpoint in H.
Step (2): None of the sets $K_{k+1}, \dots, K_m$ hits $M = H \cap \bigcup_{i=1}^k K_i$.
Step (3): D and D' are path-connected in K^C.

Clearly Step (3) contradicts the assumption that D and D' are different connected components of K^C.

To show Step (1), assume that at least one of the sets in $\{K_1, \dots, K_k\}$ contains a disk of radius $2t_1$ with midpoint in H. As $\bigcup_{i=1}^k K_i$ is connected ($K \cap [d, d']$ is a line-segment), there must be two indices $i, j \in \{1, \dots, k\}$ such that $K_i \cap K_j \neq \emptyset$, K_i contains a disk of radius $2t_1$ with midpoint in H and K_j contains a disk of radius $2t_1$ with midpoint in $\mathbb{R}^2 \setminus H$. By the definition of t_1, the intersection $K_i \cap K_j$ must contain a disk of radius $2t_1$, so at least one of the sets, say K_i, contains two disks B_1 and B_2 with midpoints on different sides of g. By convexity,

$$e = g \cap \operatorname{conv}(B_1 \cup B_2) \subset K_i,$$

where e is a line segment of length at least $4t_1$. As K_i hits $[d, d']$, this implies $e \subset [d, d']$, a contradiction.

To show Step (2), let $i \in \{1, \dots, m\}$ be such that K_i hits M. This implies that there is a point

$$y_{ij} \in K_i \cap K_j \cap H$$

for some $j \in \{1, \dots, k\}$. As K_i and K_j overlap, there is a disk $z_{ij} + 2t_1 B^2 \subset K_i \cap K_j$. By (1), $z_{ij} \notin H$. Hence $[y_{ij}, z_{ij}]$ hits g in a point $x \in K_i \cap K_j$. $x \in K_j$ implies $x \in [d, d']$ and $x \in K_i$ now gives $i \in \{1, \dots, k\}$.

We show Step (3). Step (2) implies that for all sufficiently small $\delta > 0$, the set

$$M_\delta = \Big(H \cap (M \oplus \delta B^2)\Big)$$

does not hit K outside M. The set $M_\delta \cap g$ is a line-segment $[c, c']$, where the notation is such that $c \in D$ and $c' \in D'$; see Figure 6. M_δ is a connected finite union of convex sets, so the boundary of the unbounded connected component of M_δ^C is a continuous closed curve containing c and c'. Removing $[c, c']$ from this curve (and adding the

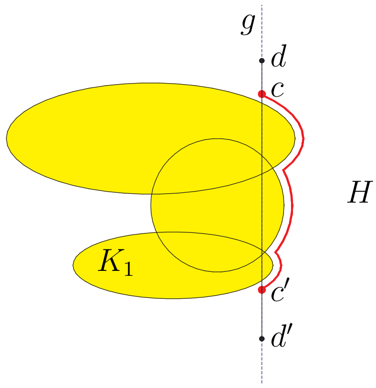

Fig. 6. The line g, spanned by $[d, d']$ together with $K_1, \ldots, K_k$ and the path connecting c and c' constructed in Step (3).

endpoints c, c'), leads to a continuous curve in K^C with endpoints c and c'. This proves Step (3) and the Lemma is shown.

Lemma 9 *Let $K \in \tilde{\mathcal{R}}$ be given. Then for $0 < \tau < t_2$ any connected component of K^C contains exactly one connected component of $(K \oplus \tau B^2)^C$ and in particular*

$$N_c(K^C) = N_c\Big((K \oplus \tau B^2)^C\Big).$$

PROOF. Let D be an arbitrary connected component of K^C. We first show that D contains at least one connected component of $(K \oplus \tau B^2)^C$, i.e. we show that $D \cap (K \oplus \tau B^2)^C$ is nonempty.

This is clear if D is unbounded, so we may assume that D is a hole of K. Let $B = z + rB^2$, $z \in D$, $r > 0$, be the largest disk contained in $\operatorname{cl} D$. Without loss of generality, assume that $K_1, \ldots, K_k$ hit ∂B, whereas $K_{k+1}, \ldots, K_m$ do not. If $r < t_2$, the definition of t_2 would imply the existence of a common point $p \in K_1 \cap \ldots \cap K_k$. For any point $x \in (\partial B) \cap K \subset K_1 \cup \ldots \cup K_k$, the segment $[x, p]$ is contained in K by convexity of the sets $K_1, \ldots, K_k$. Hence $[x, p] \cap \operatorname{int} B = \emptyset$, which implies that $(\partial B) \cap K$ must be contained in the open half plane bounded by the line $z + (p - z)^\perp$ and containing p. A small translation of B in the direction $z - p$ therefore results in a disk in D which does not touch K. This contradicts the maximality of the radius of B. We conclude that $r \geqslant t_2$ and thus, $D \cap (K \oplus \tau B^2)^C \neq \emptyset$.

As any connected component of $(K \oplus \tau B^2)^C$ must be contained in exactly one connected component of K^C, we have

$$N_c(K^C) \leqslant N_c((K \oplus \tau B^2)^C)$$

with equality if and only if each D contains exactly one connected component of $(K \oplus \tau B^2)^C$. The inclusion-exclusion principle states that

$$\chi(K) = \sum_{\emptyset \neq I \subset \{1,\ldots,m\}} (-1)^{\#I+1} \chi(K_I),$$

where $K_I := \bigcap_{i \in I} K_i$. It can be derived directly from the additivity of χ; see e.g. [20]. Applying this to K and $K \oplus \tau B^2$, we get $\chi(K) = \chi(K \oplus \tau B^2)$. Here we used $\tau < t_2$ and the fact that $\chi(K)$ of a nonempty convex set is always 1. Also, $\tau < t_2$ implies $N_c(K) = N_c(K \oplus \tau B^2)$ and thus (1) gives $N_h(K) = N_h(K \oplus \tau B^2)$. We conclude

$$N_c(K^C) = N_c((K \oplus \tau B^2)^C).$$

This shows the claim.

The following theorem is only stated for $\mathbb{L} = \mathbb{Z}^2$. By a suitable linear transformation, it extends to other regular lattices, where the bound for t in (16) must be adjusted; see the end of this section for details.

Theorem 10 *Let $\mathbb{L} = \mathbb{Z}^2$ be the standard lattice and let $K \in \tilde{\mathcal{R}}$ be given. Then*

$$\hat{N}_c(\hat{Q}_t) - 1 = N_h(K)$$

for all

$$0 < t < \min\left\{\frac{t_4}{76} t_0, 2\sqrt{2} t_1, \frac{t_2}{4}\right\}. \tag{16}$$

PROOF. By scaling with $1/t$, we may assume $t = 1$ and hence

$$1 < \min\left\{\frac{t_4}{76} t_0, 2\sqrt{2} t_1, \frac{t_2}{4}\right\}. \tag{17}$$

This implies that $\sqrt{2} < 4 < t_2$ and

$$N_h(K) = N_c(K^C) - 1 = N_c\Big((K \oplus \sqrt{2}B^2)^C\Big) - 1$$

by Lemma 9. In the following, we show

$$N_c\Big((K \oplus \sqrt{2}B^2)^C\Big) = \hat{N}_c(\hat{Q}_t). \tag{18}$$

Let D be a connected component of $(K \oplus \sqrt{2}B^2)^C$ and $z \in D$. Then $z + \sqrt{2}B^2 \subset K^C$ and the cell C which contains z is completely contained in K^C. By the definition of $\hat{Q}_1$, we find $z \in C \subset \hat{Q}_1$. This shows that $D \subset \hat{Q}_1$, so any connected component of $(K \oplus \sqrt{2}B^2)^C$ is contained in $\hat{Q}_1$. We show that different components of $(K \oplus \sqrt{2}B^2)^C$ are not connected in $\hat{Q}_1$. If C and $\tilde{C}$ are two cells in the same connected component of $\hat{Q}_1$, then there is an edge-path in $\mathcal{G}_8(K^C)$ of line segments connecting the two cells. If $\operatorname{vert} C$ and $\operatorname{vert} \tilde{C}$ would hit different connected components of K^C, there would be an edge with starting point in one connected component and endpoint in another. But this contradicts Lemma 8, as the length of the edge is at most $\sqrt{2} < 4t_1$. We therefore have $N_c\Big((K \oplus \sqrt{2}B^2)^C\Big) \leqslant \hat{N}_c(\hat{Q}_1)$.

To prove $N_c\Big((K \oplus \sqrt{2}B^2)^C\Big) \geqslant \hat{N}_c(\hat{Q}_1)$, it is enough to to show that for any cell C in $\hat{Q}_1$ that hits a connected component D of K^C there is an edge path from $\operatorname{vert} C$

to $D \cap (K \oplus \sqrt{2}B^2)^C$. The latter set is connected by Lemma 12. As before, this edge path cannot leave the component it started in, so we only have to show that it ends in $(K \oplus \sqrt{2}B^2)^C$. This is shown in the Lemma 11, below, and completes the proof.

Lemma 11 *Let $\mathbb{L} = \mathbb{Z}^2$ and $K \in \tilde{\mathcal{R}}$ be given. If*

$$1 < \min\left\{\frac{t_4}{76}t_0, \frac{t_2}{4}\right\} \tag{19}$$

and $C = x + \mathsf{C}_0$, $x \in \mathbb{L}$, is a cell with all its vertices in K^C, then there is an edge path in $\mathcal{G}_8(K^C)$ from a vertex of C to a point in $(K \oplus \sqrt{2}B^2)^C$.

PROOF. Let a be the midpoint of C. The disk B_0 with radius $76/t_4$ centered at a, does hit at most two sets in $\{K_1, \dots, K_m\}$, due to (19). Without loss of generality, we may assume that $B_0 \cap K = B_0 \cap (K_1 \cup K_2)$. The required edge path will be constructed within B_0 and therefore only has to avoid the two sets K_1 and K_2. Due to (13), the radius of B_0 is at least 152, which implies that short edge paths starting at an edge of C (e.g. of length 2 or 5, as constructed below) will be contained in B_0. Let v_1, v_2, v_3, v_4 be the vertices of C in counterclockwise order and let V_j be the closed normal cone of v_j translated with v_j, $j = 1, 2, 3, 4$; see Figure 7. By convexity of K_1, two of these cones cannot contain any point of K_1, and the same holds true for K_2. Re-indexing leads to the following three cases:

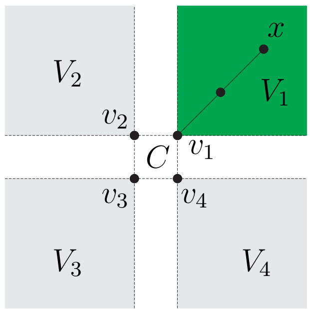

Fig. 7. The normal cones of the vertices of C. The conditions in the first treated case imply that V_1 (the dark-gray area) does not hit $K_1 \cup K_2$.

1st case: K_1 and K_2 do not hit V_j for at least one $j = 1, \dots, 4$. We assume $j = 1$ and can construct an edge path of Euclidean length $2\sqrt{2}$, whose endpoint x has a distance larger than $\sqrt{2}$ from $K_1 \cup K_2$ and hence from K. It is therefore in $(K \oplus \sqrt{2}B^2)^C$, as required; see Figure 7.

2nd case: $K_1 \cap V_1 = K_1 \cap V_3 = \emptyset$ and $K_2 \cap V_2 = K_2 \cap V_4 = \emptyset$; see Figure 8, left. As V_1 is convex and the convex body K_1 does not hit it, there is a supporting line g through the vertex v_1 of V_1, that strictly separates V_1 and K_1. If necessary, we can reflect at the diagonal of V_1, and re-index the sets, to guarantee that the point $v_1 + (-1, 1)$ and V_1 are on the same side of g. Let V_1' be the smallest cone with apex v_1 containing $v_1 + (-1, 1)$ and V_1. By construction, $V_1' \cap K_1 = \emptyset$ and thus, we can construct a path outside $K_1 \cup K_2$ whose endpoint x does not hit $(K_1 \cup K_2) \oplus \sqrt{2}B^2$;

see Figure 8, right. As this path is contained in B_0, we conclude $x \in (K \oplus \sqrt{2}B^2)^C$, as required.

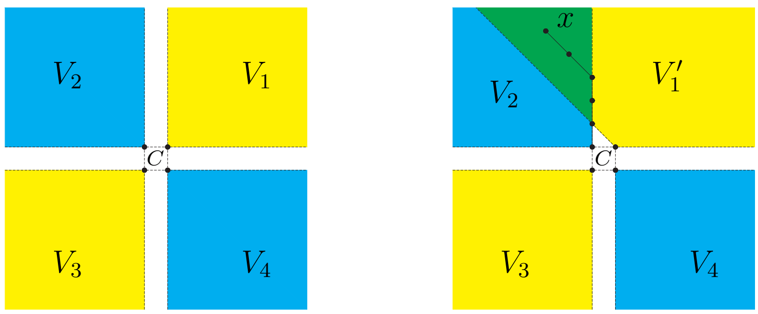

Fig. 8. On the left, the assumptions of the 2nd case are illustrated: The light-gray cones do not hit K_1, the medium gray cones do not hit K_2. On the right, V_1 is extended to a cone V_1' that does not hit K_1 thus producing a dark gray area not hitting $K_1 \cup K_2$. A path with endpoint x is indicated.

3rd case: $K_1 \cap V_1 = K_1 \cap V_2 = \emptyset$ and $K_2 \cap V_3 = K_2 \cap V_4 = \emptyset$. This is the most involved case. We first construct a point $p \in K_1 \cap K_2$ close to C using Lemma 6. In analogy to the first case, a desired path can be constructed if one of the two disks $x_1 + \sqrt{2}B^2$, $x_2 + \sqrt{2}B^2$ (the points x_1, x_2 are defined as the endpoints of "diagonal paths" of Euclidean length $2\sqrt{2}$, see Figure 9, left) is disjoint with K_2. We may therefore assume that both contain a point of K_2 and thus there is a point $w_2 \in K_2$ on the horizontal line through v_2 with $\|w_2 - v_2\| \leqslant 2 + \sqrt{2}$. An analogue construction in the lower half plane yields a point $w_1 \in K_1$ on the same line with $\|w_1 - v_3\| \leqslant 2 + \sqrt{2}$. As $\|w_1 - w_2\| \leqslant 5 + 2\sqrt{2} < 8$, we have

$$(K_1 \oplus 4B^2) \cap (K_2 \oplus 4B^2) \neq \emptyset,$$

which implies $K_1 \cap K_2 \neq \emptyset$, as $t_2 > 4$ by (19). This implies $\operatorname{int}(K_1 \cap K_2) \neq \emptyset$, as $K \in \tilde{\mathcal{R}}$. Lemma 6 can now be applied with v_1, v_2 replaced by w_1, w_2, respectively, where we use that $[w_1, w_2] \not\subset K_1 \cup K_2$, as $[w_1, w_2]$ contains v_3: there is a point $p \in K_1 \cap K_2$ with

$$\max\{\|p - w_1\|, \|p - w_2\|\} \leqslant 8 \frac{D(K_1, K_2)}{2t_1(K_1, K_2)} \leqslant \frac{8}{t_4}.$$

By (13), this gives

$$\|p - a\| \leqslant \|p - w_1\| + \|w_1 - v_3\| + \|v_3 - a\| \leqslant \frac{8}{t_4} + 5 \leqslant \frac{21}{2t_4} = \rho, \tag{20}$$

say. Note that $p \notin V_1 \cup \ldots \cup V_4$, so p is an element of the white, cross-shaped area in Figure 9, left.

For the last step of the proof, we may assume without loss of generality that the most distant point in $\operatorname{vert} C$ to p is v_1. This and (20) imply that $p \in Q$, where Q is the union of two squares whose axis-parallel sides have length $1/2$ and ρ, cf. Figure 9, right. As $v_1 \notin K_2$, there is a closed half-space containing K_2 such that

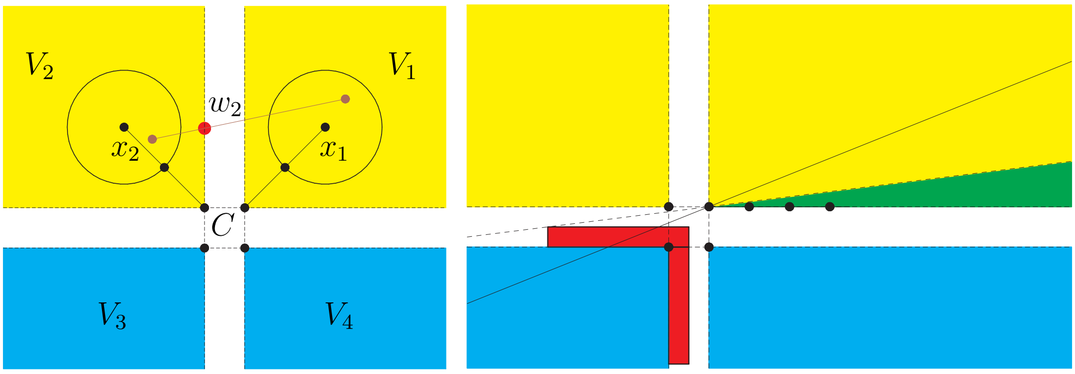

Fig. 9. On the left, the 3rd case is illustrated: The light gray cones do not hit K_1, the medium gray cones do not hit K_2. A point $w_2 \in K_2$ is constructed whose distance from C is at most $2+\sqrt{2}$. On the right, a possible line g and the dark gray set Q are shown. The wedge in the lower part of V_1 does not hit $K_1 \cup K_2$.

its bounding line g contains v_1. g cannot be vertical, as we have already excluded $K_2 \cap V_1 = \emptyset = K_2 \cap V_2$. For the same reason, K_2 must be contained in the half plane above g. In particular, $p \in Q$ is above g. Thus the slope of g is at least

$$\frac{1/2}{1/2+\rho} \geqslant \frac{2t_4}{43}. \tag{21}$$

Define a path starting at v_1 and walking n steps to the right and subsequently two steps upward and call its endpoint x. Due to (21), the path cannot hit $K_1 \cup K_2$ and we have $(K_1 \cup K_2) \cap (x+\sqrt{2}B^2) = \emptyset$, provided that $n \geqslant 74/t_4$. The choice of $74/t_4 \leqslant n < 74/t_4 + 1$ yields in addition

$$\sqrt{2} + \|x-a\| = \sqrt{2} + \sqrt{\left(2+\frac{1}{2}\right)^2 + \left(n+\frac{1}{2}\right)^2} < \frac{76}{t_4}$$

so the definition of the radius of B_0 implies that $x+\sqrt{2}B^2$ and the path both are subsets of B_0. This shows that $x+\sqrt{2}B^2$ and the path do not hit K. The conclusion that $x \in (K \oplus \sqrt{2}B^2)^C$ finishes the considerations for the third case.

We mention how Theorem 10 can be extended to non-standard lattices. Let $\mathbb{L}$ be a lattice generated by a basis x_1, x_2. Put $r = \min\{\|x_1\|, \|x_2\|\}$, $R = \max\{\|x_1\|, \|x_2\|\}$, and $\gamma = |\cos \sphericalangle(x_1, x_2)|$, where $\sphericalangle(x_1, x_2)$ is the (smaller) angle between x_1 and x_2. Let $\Phi : \mathbb{R}^2 \longrightarrow \mathbb{R}^2$ be the linear mapping that maps the standard basis (e_1, e_2) to the basis (x_1, x_2). The image of B^2 under Φ is an ellipse which satisfies

$$r\sqrt{1-\gamma}B^2 \subset \Phi(B^2) \subset R\sqrt{1+\gamma}B^2. \tag{22}$$

In other words, the length of the image of a unit segment under Φ is at least $r\sqrt{1-\gamma}$ and at most $R\sqrt{1+\gamma}$. If $K = \bigcup_{i=1}^m K_i$ is a representation of K satisfying the conditions (i) and (ii) in the definition in of $\tilde{\mathcal{R}}$, then $\bigcup_{i=1}^m \Phi^{-1}(K_i)$ is such a representation for $\tilde{K} = \Phi^{-1}(K)$ This shows that we may assume $\mathbb{L} = \mathbb{Z}^2$, $x_1 = e_1, x_2 = e_2$, $\mathsf{C}_0 = [0,1]^2$ and work with $\tilde{K}$. The constants $\tilde{t}_0$, $\tilde{t}_1$ $\tilde{t}_2$, and $\tilde{t}_4$ of $\tilde{K}$ with respect to the above representation satisfy

$$\tilde{t_0} \geqslant \frac{t_0}{R\sqrt{1+\gamma}}, \qquad \tilde{t_1} \geqslant \frac{t_1}{R\sqrt{1+\gamma}}, \qquad \tilde{t_2} \geqslant \frac{t_2}{R\sqrt{1+\gamma}}, \qquad \tilde{t_4} \geqslant \frac{r\sqrt{1-\gamma}}{R\sqrt{1+\gamma}} t_4$$

due to (22). This can be substituted in the condition for t in Theorem 10 to obtain a bound in terms of the representation of K.

Theorem 1 is now a direct consequence of Theorems 7 and 10.

References

[1] R.W. Boyce, D.C. Ebert, T.A. Youngs, C.L. Paddock, Li. Mosekilde, M.L. Stevens, H.J.G. Gundersen, *Unbiased estimation of vertebral trabecular connectivity in calcium-restricted ovariectomized minipigs*, Bone **16** (1995) 637–642.

[2] K.R. Mecke, A morphological model for complex fluids, *J. Phys.: Condens. Matter* **8** (1996) 9663–9667.

[3] P.E. Levitz, Generic methods for the characterization of porous materials, in: F. Schüth, K.S.W. Sing, J. Weitkamp. (Eds.) *Handbook of Porous Solids*, **1**, Wiley–VCH, Weinheim (2002) 37–80.

[4] R. Schneider, W. Weil, *Stochastische Geometrie*, Teubner, Stuttgart (2000).

[5] R. Klette, A. Rosenfeld, *Digital Geometry*, Elsevier, New York (2004).

[6] J. Serra, *Image Analysis and Mathematical Morphology*, Vol. 1, Academic Press, London (1982).

[7] A. Rosenfeld, A. Kak, *Digital Picture Processing*, Academic Press, New York (1979).

[8] H.J.A.M. Heijmans, *Morphological image operators*, Academic Press, New York (1994).

[9] J. Ohser, W. Nagel, K. Schladitz, The Euler number of discretized sets – on the choice of adjacency in homogeneous lattices, *Lecture Notes in Physics* **600** (2002) 275 - 298.

[10] J. Ohser, W. Nagel, K. Schladitz, The Euler number of discretised sets – surprising results in three dimensions, *Image Anal. Stereol.* **22** (2003) 11–19.

[11] C. Lee, T. Poston, A. Rosenfeld, Winding and Euler Numbers for 2D and 3D Digital Images, CVGIP: *Graph. Models Image Proc.* **53** (1991) 522–537.

[12] J. Ohser, W. Nagel, The estimation of the Euler-Poincaré characteristic from observations in parallel sections, *J. Microsc.* **184** (1995) 117–126.

[13] H. Hadwiger, *Vorlesungen über Inhalt, Oberfläche und Isoperimetrie*, Springer, Berlin (1957).

[14] I.S. Molchanov, *Statistics of the Boolean Models for Practitioners and Mathematicians*, Wiley, Chichester (1996).

[15] M. Kiderlen, Estimation of the specific Euler characteristic of a planar Boolean model from digitizations, *in preparation* (2006+).

[16] J. Ohser, F. Mücklich, *Statistical analysis of microstructures in materials science*, J. Wiley, New York (2000).

[17] H. Bieri, W. Nef, Algorithms for the Euler characteristic and related additive functionals of digital objects, *Comput. Graphics Image Process.* **28** (1984) 166–175.

[18] Ch.R. Dyer, Computing the Euler number of an image from its quadtree, *Comput. Graphics Image Process.* **13** (1980) 270–276.

[19] A. Rosenfeld, J.L. Pfaltz, Sequential operations in digital picture processing, *J. ACM* **13** (1966) 471–494.

[20] R. Schneider, *Convex Bodies: The Brunn-Minkowski Theory*, Cambridge Univ. Press, Cambridge (1993).

[21] D.B. West, *Introduction to Graph Theory* Englewood Cliffs, NJ: Prentice Hall (1996).